Accurate Determination of Magnetic Field Gradients from Four Point Vector Measurements—Part I: Use of Natural Constraints on Vector Data Obtained From a Single Spinning Spacecraft

Emil L. Kepko, Krishan K. Khurana, Margaret G. Kivelson, Richard C. Elphic, and Christopher T. Russell

Abstract—**Cluster introduces a new generation of spacecraft that will measure the spatial gradients of the magnetic field in the Earth's magnetosphere. As gradients require knowledge of differences, small errors resulting from an inadequate knowledge of the orientations, zero levels and the scale factors of the magnetometer sensors affect the calculation of field gradients disproportionately and must be removed with high accuracy. We show that twelve calibration parameters are required for each of the spacecraft (for a total of 48 for the four spacecraft) to correctly infer the measured magnetic fields at each of the spacecraft.**

By application of a Fourier transform technique, some of the parameters can be recovered. We will show that errors in eight of the twelve calibration parameters generate coherent monochromatic signals at the first and the second harmonics of the spin frequency in the despun data. These narrow-band signals can be readily characterized because of the natural constraint that low frequency geophysical signals in the Earth's magnetosphere have a broad-band character. We relate the real and the imaginary parts of the monochromatic signals to the eight calibration parameters. We then present a least squares scheme that improves the eight calibration parameters by iteration until the power of the coherent signal superimposed above the broad-band background is minimized. In an accompanying paper, we report on another technique that determines the rest of the calibration parameters by utilizing the natural constraints that $\nabla \cdot B$ is zero everywhere and $\nabla \times B$ is vanishingly small in certain regions of the magnetosphere.

I. Introduction

A PRINCIPAL objective of the multispacecraft mission Cluster is the direct measurement of the spatial gradients of the magnetic field throughout the magnetosphere [1], [2]. The measurement accuracy needed to understand physical processes operating in the Earth's magnetosphere places very stringent requirements on the reliability of the measured magnetic field. The first-differences (the differences in the values of a field component measured at two locations) are typically very small compared to the background field. Errors arise from uncertainty in the absolute orientations of the sensors (misorientation), the offsets (misleveling), and the sensor gains (improper scaling); these uncertainities are often comparable in size with the first-order differences. For example, if a sensor assembly on a spacecraft is misaligned by an angle $\Delta\alpha$ with respect to the sensor assemblies on another spacecraft, the resulting error in $\nabla \times \boldsymbol{B}$ can be as large as $B_0 \sin \Delta\alpha/d$, where B_0 is the value of the background field and d is the spacecraft spacing. Thus, for an average spacecraft spacing of 1000 km, a misalignment between two different sensor assemblies by one degree can result in an error of as much as 2.2 nT/R_E in $\nabla \times \boldsymbol{B}$ in a background field of 20 nT. If the separation between the spacecraft were 500 km, the peak error in $\nabla \times \boldsymbol{B}$ could be as large as 4.4 nT/R_E. For reference, the peak values of $\nabla \times \boldsymbol{B}$ in the Earth's current sheet in the magnetotail near $X = -15\ R_E$ are of order 15 nT/R_E.

The calibration of a single, near-orthogonal sensor triad requires the determination of twelve quantities. These could be thought of as the nine elements of a coupling matrix (C) that orthogonalizes, scales and correctly orients the sensor data and the three offsets (O) that correct for the zero levels of the sensors. Thus,

$$\begin{pmatrix} B_x \\ B_y \\ B_z \end{pmatrix} = \begin{pmatrix} c_{11} & c_{12} & c_{13} \\ c_{21} & c_{22} & c_{23} \\ c_{31} & c_{32} & c_{33} \end{pmatrix} \begin{pmatrix} B_{S_1} - O_1 \\ B_{S_2} - O_2 \\ B_{S_3} - O_3 \end{pmatrix} \quad (1)$$

In this and an accompanying paper [3], we introduce new techniques to fully correct or compensate for all of the 48 calibration parameters. In this work, we develop a Fourier transformed-based technique to recover eight of the twelve calibration parameters for each of the spacecraft by using the natural constraint that low-frequency geophysical signals in the Earth's magnetosphere have a broad-band character. In the accompanying paper [3], we report on another technique that determines the rest of the calibration parameters by utilizing the natural constraints that $\nabla \cdot \boldsymbol{B}$ is zero everywhere and $\nabla \times \boldsymbol{B}$ is vanishingly small

Manuscript received May 8, 1995. This work was supported by the National Aeronautics and Space Administration Division of Space Physics under Grant NAG5-1167. UCLA-IGPP publication number 4281.

The authors are with the Institute of Geophysics and Planetary Physics, Slichter Hall, University of California at Los Angeles, Los Angeles, CA 90024.

Publisher Item Identifier S 0018-9464(95)00645-0.

TABLE I
SUMMARY OF THE COORDINATE SYSTEMS USED IN THIS PAPER

notation	coordinate system
X, Y, Z	Despun spacecraft coordinate system (orthogonal)
X', Y', Z'	Despun pseudo-spacecraft coordinate system (non-orthogonal)
x, y, z	Spinning spacecraft coordinate system (orthogonal)
S_1, S_2, S_3	Spinning sensor coordinate system (non - orthogonal)

in certain regions of the magnetosphere. Results of calibrations performed on data obtained from the ISEE mission are also presented.

II. Coordinate Systems

In our papers, we will have occasion to express the vector magnetic field in four different coordinate systems. We begin with the orthogonal spinning spacecraft coordinate system (x, y, z) which rotates with the spacecraft. The z-axis of this coordinate system is parallel to the spin axis of the spacecraft, and the x- and y-axes lie in the spin plane of the spacecraft with y-axis leading the x-axis by 90° in the direction of rotation. The three sensors S_1, S_2, and S_3 point roughly along the x, y, and z directions of the spacecraft, respectively. The sensor coordinate system (S_1, S_2, S_3) spins with the spacecraft, but because of individual sensor misalignments is not necessarily an orthogonal coordinate system. The actual measurements onboard the spacecraft are made in this coordinate system. By applying a despin matrix, the data from the two rotating coordinate systems can be transformed into two despun coordinate systems: one orthogonal and the other nonorthogonal. The orthogonal despun spacecraft coordinate system is denoted by (X, Y, Z), whereas the despun nonorthogonal coordinate system (called the despun pseudospacecraft coordinate system) is denoted by (X', Y', Z'). Table I provides a summary of the four coordinate systems.

III. Basic Equations

A vector pointed along a sensor S can be related to the three orthogonal components directed along the spinning spacecraft coordinates (x, y, z) through the relation

$$B_S = B_x \sin\theta \cos\varphi + B_y \sin\theta \sin\varphi + B_z \cos\theta \qquad (2)$$

where θ is the elevation angle of the sensor with respect to the z-axis and φ is the azimuthal angle the projection of the sensor makes with the x-axis in the x-y plane.

The measurements made by the sensors may also have small offsets because of the magnetic fields generated by the spacecraft subsystems, or because the zero levels of the sensors have drifted over time. The gain factors of the sensors may also have changed since the ground calibrations because of aging. Thus, the measurements provided by the sensors are related to the actual background field in spacecraft coordinates through

$$\begin{pmatrix} (B_{S_1} - O_1)/G_1 \\ (B_{S_2} - O_2)/G_2 \\ (B_{S_3} - O_3)/G_3 \end{pmatrix} = \begin{pmatrix} \sin\theta_1 \cos\varphi_1 & \sin\theta_1 \sin\varphi_1 & \cos\theta_1 \\ \sin\theta_2 \cos\varphi_2 & \sin\theta_2 \sin\varphi_2 & \cos\theta_2 \\ \sin\theta_3 \cos\varphi_3 & \sin\theta_3 \sin\varphi_3 & \cos\theta_3 \end{pmatrix} \begin{pmatrix} B_x \\ B_y \\ B_z \end{pmatrix}. \qquad (3)$$

Equation (3) can be rearranged so that only the sensor measurements appear on the left-hand side of the equation

$$\begin{pmatrix} B_{S_1} \\ B_{S_2} \\ B_{S_3} \end{pmatrix} = \begin{pmatrix} G_1 \sin\theta_1 \cos\varphi_1 & G_1 \sin\theta_1 \sin\varphi_1 & G_1 \cos\theta_1 \\ G_2 \sin\theta_2 \cos\varphi_2 & G_2 \sin\theta_2 \sin\varphi_2 & G_2 \cos\theta_2 \\ G_3 \sin\theta_3 \cos\varphi_3 & G_3 \sin\theta_3 \sin\varphi_3 & G_3 \cos\theta_3 \end{pmatrix} \cdot \begin{pmatrix} B_x \\ B_y \\ B_z \end{pmatrix} + \begin{pmatrix} O_1 \\ O_2 \\ O_3 \end{pmatrix}. \qquad (4)$$

The matrix on the right-hand side of the equation is often called the orthogonality matrix because it contains information on the orthogonality of the sensors. For a perfectly calibrated sensor triad, the orthogonality matrix would reduce to a unitary matrix. The coupling matrix of equation (1) is the inverse of the orthogonality matrix.

As the actual background field (B_x, B_y, B_z) is not known, (4) cannot be solved by using the standard matrix inversion schemes. However, we will show below that if the raw sensor data (B_{S_1}, B_{S_2}, B_{S_3}) are transformed into an inertial frame by applying a despin matrix, the resulting data possess coherent monochromatic signals at the first and the second harmonics of the spin frequency of the spacecraft. The calibration parameters can be related to the first and second harmonics through a set of linearized equations which can then be solved to obtain some of the calibration parameters.

Equation (4) can be simplified by measuring the elevation and azimuthal angles of the sensors with respect to the nearest spacecraft coordinate axis, that is,

$$\theta_1 = 90 - \Delta\theta_1 \qquad \theta_2 = 90 - \Delta\theta_2 \qquad \theta_3 = \Delta\theta_3$$
$$\varphi_1 = \Delta\varphi_1 \qquad \varphi_2 = 90 + \Delta\varphi_2 \qquad \varphi_3 = \varphi_3 \qquad (5)$$

where the elevation angles $\Delta\theta_1$ and $\Delta\theta_2$ are measured from the x-y plane, $\Delta\theta_3$ is measured with respect to the z-axis, $\Delta\varphi_1$ and φ_3 are measured from the x-axis, and $\Delta\varphi_2$ is measured from the y-axis. Notice that with the exception of φ_3, all of the angles are expected to be small. Thus, we use the small angle approximation $\cos\Delta\alpha \approx 1$ and $\sin$

$\Delta\alpha \approx \Delta\alpha$, and get

$$\begin{pmatrix} B_{S_1} \\ B_{S_2} \\ B_{S_3} \end{pmatrix} = \begin{pmatrix} G_1 & G_1\Delta\varphi_1 & G_1\Delta\theta_1 \\ -G_2\Delta\varphi_2 & G_2 & G_2\Delta\theta_2 \\ G_3\Delta\theta_3\cos\varphi_3 & G_3\Delta\theta_3\sin\varphi_3 & G_3 \end{pmatrix} \cdot \begin{pmatrix} B_x \\ B_y \\ B_z \end{pmatrix} + \begin{pmatrix} O_1 \\ O_2 \\ O_3 \end{pmatrix}. \tag{6}$$

The gain factors in the above equation are numbers close to unity. We further use the simplification that

$$\begin{aligned} G_2 &= G_1 + \Delta G_{21} \\ \Delta\varphi_2 &= \Delta\varphi_1 + \Delta\varphi_{21}. \end{aligned} \tag{7}$$

Notice that $\Delta\varphi_{21} = \Delta\varphi_2 - \Delta\varphi_1 = 90° - (\varphi_2 - \varphi_1)$ is a measure of the nonorthogonality of the spin plane sensors, and ΔG_2 is a measure of the nonequality of their gains. The implications of substitutions (7) will become apparent later in the work. Ignoring second-order terms, we get

$$\begin{pmatrix} B_{S_1} \\ B_{S_2} \\ B_{S_3} \end{pmatrix} = \begin{pmatrix} G_1 & G_1\Delta\varphi_1 & G_1\Delta\theta_1 \\ -G_1(\Delta\varphi_1 + \Delta\varphi_{21}) & G_1 + \Delta G_{21} & G_1\Delta\theta_2 \\ G_3\Delta\theta_3\cos\varphi_3 & G_3\Delta\theta_3\sin\varphi_3 & G_3 \end{pmatrix} \cdot \begin{pmatrix} B_x \\ B_y \\ B_z \end{pmatrix} + \begin{pmatrix} O_1 \\ O_2 \\ O_3 \end{pmatrix}. \tag{8}$$

A similar linearized form for the relationship between the sensor fields and the background field, omitting effect of incorrect gain factors, was obtained by Farrell *et al.* [4].

The data in the spinning spacecraft coordinate system and the despun spacecraft coordinate system are related by

$$\begin{aligned} B_x &= B_H\cos(\omega t - \psi) \\ B_y &= -B_H\sin(\omega t - \psi) \\ B_z &= B_Z \end{aligned} \tag{9}$$

where $B_H = \sqrt{B_X^2 + B_Y^2}$ is the magnitude of the field in the X-Y plane, and $\psi = \tan^{-1}(B_Y/B_X)$ is the angle that the projection of the magnetic field in the spin plane makes with the X-axis. By multiplying both sides of (8) with the despin matrix

$$D = \begin{pmatrix} \cos\omega t & -\sin\omega t & 0 \\ \sin\omega t & \cos\omega t & 0 \\ 0 & 0 & 1 \end{pmatrix} \tag{10}$$

we get

$$\begin{aligned} B_{X'} = {} & G_1B_H(\cos\psi + \Delta\varphi_2\sin\psi) \\ & + G_1\frac{B_H}{2}(\Delta G'_{21}\cos\psi - \Delta\varphi_2\sin\psi) \\ & + \cos\omega tG_1(B_z\Delta\theta_1 + O'_1) \\ & + \sin\omega tG_1(-B_z\Delta\theta_2 - O'_2) \\ & + \cos2\omega tG_1\frac{B_H}{2}(-\Delta G'_{21}\cos\psi - \Delta\varphi_{21}\sin\psi) \\ & + \sin2\omega tG_1\frac{B_H}{2}(-\Delta G'_{21}\sin\psi + \Delta\varphi_{21}\cos\psi) \end{aligned} \tag{11a}$$

$$\begin{aligned} B_{Y'} = {} & G_1B_H(\sin\psi - \Delta\varphi_2\cos\psi) \\ & + G_1\frac{B_H}{2}(\Delta G'_{21}\sin\psi + \Delta\varphi_2\cos\psi) \\ & + \cos\omega tG_1(B_z\Delta\theta_2 + O'_2) \\ & + \sin\omega tG_1(B_z\Delta\theta_1 + O'_1) \\ & + \cos2\omega tG_1\frac{B_H}{2}(\Delta G'_{21}\sin\psi - \Delta\varphi_{21}\cos\psi) \\ & + \sin2\omega tG_1\frac{B_H}{2}(-\Delta G'_{21}\cos\psi - \Delta\varphi_{21}\sin\psi) \end{aligned} \tag{11b}$$

$$\begin{aligned} B_{Z'} = {} & G_3(B_z + O'_3) \\ & + \cos\omega tG_3B_H(\cos\varphi_3\Delta\theta_3\cos\psi + \sin\varphi_3\Delta\theta_3\sin\psi) \\ & + \sin\omega tG_3B_H(-\sin\varphi_3\Delta\theta_3\cos\psi + \cos\varphi_3\Delta\theta\sin\psi) \end{aligned} \tag{11c}$$

where we have defined

$$O'_3 = \frac{O_3}{G_3} \quad O'_1 = \frac{O_1}{G_1} \quad O'_2 = \frac{O_2}{G_1} \quad \text{and} \quad \Delta G'_{21} = \frac{\Delta G_{21}}{G_1}. \tag{12}$$

Equation (11a)–(11c) form the basis of the calibration procedure. They relate the errors in calibration parameters to the coherent monochromatic signals in the despun data at the first and the second harmonics of the spin frequency of the spacecraft. From these equations, we learn that the elevation of S_1 and S_2 out of the spin plane ($\Delta\theta_1$ and $\Delta\theta_2$) and the offsets O_1 and O_2 in the spin plane sensors produce first harmonic signatures in $B_{X'}$ and $B_{Y'}$ (through their association with the $\sin\omega t$ and $\cos\omega t$ terms). The nonorthogonality of the spin plane sensors ($\Delta\varphi_{21}$) and the mismatch of the gains (ΔG_{21}) generate signals at the second harmonic in $B_{X'}$ and $B_{Y'}$. We also learn that the elevation ($\Delta\theta_3$) of the spin axis sensor from the z-axis generates a first harmonic in $B_{Z'}$. Finally, we learn that three

of the calibration parameters (G_3, φ_1, O_3) are not associated either with the first or the second harmonic terms, and thus do not produce coherent spin-related signals in the despun data. The calibration parameter G_1 does appear in association with first and second harmonic terms, but always occurs in association with other calibration parameters. These four parameters cannot be determined by methods that relate to the power in the spin tones. From now on, we will assume that fairly reliable values of these four parameters are available from ground calibrations. In an accompanying paper, we will describe how these parameters can be refined further.

By Fourier transforming both sides of (11a)–(11c) through the relation

$$F(\omega) = 1/T \int_0^T f(t)e^{-i\omega t}\, dt \tag{13}$$

we resolve the three time series into their Fourier components

$$B_{X'}(\omega = 0) = B_H G_1 \cos\psi + \frac{B_H}{2} G_1(\Delta G'_{21} \cos\psi + \Delta\varphi_{21} \sin\psi) \tag{14a}$$

$$\Re\{B_{X'}(\omega = \omega_{sp})\} = G_1(B_z\Delta\theta_1 + O'_1) \tag{14b}$$

$$\Im(B_{X'}(\omega = \omega_{sp})\} = G_1(-B_z\Delta\theta_2 - O'_2) \tag{14c}$$

$$\Re\{B_{X'}(\omega = 2\omega_{sp})\} = G_1 \frac{B_H}{2}(-\Delta G'_{21} \cos\psi - \Delta\varphi_{21} \sin\psi) \tag{14d}$$

$$\Im\{B_{X'}(\omega = 2\omega_{sp})\} = G_1 \frac{B_H}{2}(-\Delta G'_{21} \sin\psi + \Delta\varphi_{21} \cos\psi) \tag{14e}$$

$$B_{Y'}(\omega = 0) = B_H G_1 \sin\psi + \frac{B_H}{2} \cdot G_1(\Delta G'_{21} \sin\psi - \Delta\varphi_{21} \cos\psi) \tag{15a}$$

$$\Re(B_{Y'}(\omega = \omega_{sp})\} = G_1(B_z\Delta\theta_2 + O'_2) \tag{15b}$$

$$\Im\{B_{Y'}(\omega = \omega_{sp})\} = G_1(B_z\Delta\theta_1 + O'_1) \tag{15c}$$

$$\Re\{B_{Y'}(\omega = 2\omega_{sp})\} = G_1 \frac{B_H}{2}(\Delta G'_{21} \sin\psi - \Delta\varphi_{21} \cos\psi) \tag{15d}$$

$$\Im\{B_{Y'}(\omega = 2\omega_{sp})\} = G_1 \frac{B_H}{2}(-\Delta G'_{21} \cos\psi - \Delta\varphi_{21} \sin\psi) \tag{15e}$$

$$B_{Z'}(\omega = 0) = G_3(B_z + O'_3) \tag{16a}$$

$$\Re\{B_{Z'}(\omega = \omega_{sp})\} = G_3 B_H(\cos\varphi_3\Delta\theta_3 \cos\psi + \sin\varphi_3\Delta\theta_3 \sin\psi) \tag{16b}$$

$$\Im\{B_{Z'}(\omega = \omega_{sp})\} = G_3 B_H(-\cos\varphi_3\Delta\theta_3 \sin\psi + \sin\varphi_3\Delta\theta_3 \cos\psi) \tag{16c}$$

where we have assumed that B_H and ψ (and therefore B_X and B_Y) are constant for the time duration (typically a few minutes) over which the Fourier transform was performed. In general, this condition is not fully met and, as a result, a background level power is present at all frequencies, superimposed on the three frequencies (0, ω, and 2ω) we are most interested in. We will discuss below how this background can be dealt with. Equations (14)–(16) express the relationships between the calibration parameters and the real and imaginary parts of the zero, first and second spin harmonics present in the despun magnetic vectors. In the next section, we discuss how this near-linear system of equations can be inverted for the calibration parameters.

IV. Least Squares Inversion

A closer examination of the above 13 equations shows that they can be conveniently assembled into five groups. The first group consists of (14a), (15a), and (16a) which can be rewritten as

$$B_{X'}(\omega = 0) = G_1 B_H \cos\psi + \Delta B_X \tag{17a}$$

$$B_{Y'}(\omega = 0) = G_1 B_H \sin\psi + \Delta B_Y \tag{17b}$$

$$B_{Z'}(\omega = 0) = G_3(B_Z + O'_3). \tag{17c}$$

Noting that $B_X = B_H \cos\psi$ and $B_Y = B_H \sin\psi$, and ignoring small contributions from the first-order quantities, we find that the three zeroth-order harmonics yield estimates of the average field in the X, Y, and Z directions. The estimates of B_X, B_Y, and B_Z are needed in solving other equations.

The second group of equations comprises (14b) and (15c) which can be rewritten in the form

$$U = B_Z\Delta\theta_1 + O'_1 \tag{18}$$

where the dependent variable U is a super set of the quantities $\Re\{B_{X'}(\omega = \omega_{sp})\}/G_1$ and $\Im\{B_{Y'}(\omega = \omega_{sp})\}/G_1$, and the independent variable B_z is obtained from (17c) under the assumption that G_3 and O'_3 are known from ground calibrations. The least squares solution of this set of equations is obtained from normal equations derived by minimizing the rms difference between the two sides of (18). We would like to point out that the inversion at this stage does not yield the best estimates of $\Delta\theta_1$ and O'_1 because nonlinear terms for calibration parameters were neglected in deriving the final equations. We therefore improve upon the estimates of these calibration parameters by adopting an iterative approach. After all of the calibration parameters have been obtained, we use the exact nonlinear form

TABLE II
CALIBRATION PARAMETERS DETERMINED FOR THE ISEE-2 SENSOR ASSEMBLY BY USING THE FOURIER TRANSFORM TECHNIQUE

$\Delta\theta_1$	$\Delta\theta_2$	$\Delta\theta_3$	$\Delta\varphi_{21}$	ΔG_{21}	φ_3	O_1	O_2
-1.41°	-0.39°	1.38°	1.05°	-0.012	-1.44°	0.12 nT	0.11 nT

of the orthogonality matrix in (4) to calculate the coupling matrix of (1). The coupling matrix is then applied to the sensor data, and these corrected data become the input for the second iteration. The corrections to the calibration parameters obtained from the second iteration are added to the values of the parameters obtained from the first iteration. This iterative procedure is repeated until no improvements are obtained in the calibration parameters (typically 4 to 5 steps).

The third group of equations comprises (14c) and (15b) which can be combined into

$$V = B_Z\Delta\theta_2 + O_2'. \tag{19}$$

Equation (19) can be solved for $\Delta\theta_2$ and O_2' in a manner similar to (18).

The fourth group of equations comprises (14d), (14e), (15d), and (15e) which can be rewritten in the form

$$W_{j=1\cdots4} = \Delta G_{21}'\alpha_j + \Delta\varphi_{21}\beta_j \tag{20}$$

where

$$W_1 = 2\Re\{B_{X'}(\omega = 2\omega_{sp})\}/(G_1B_H),$$
$$\alpha_1 = -\cos\psi, \quad \beta_1 = -\sin\psi$$
$$W_2 = 2\Im\{B_{X'}(\omega = 2\omega_{sp})\}/(G_1B_H),$$
$$\alpha_2 = -\sin\psi, \quad \beta_2 = \cos\psi$$
$$W_3 = 2\Re\{B_{Y'}(\omega = 2\omega_{sp})\}/(G_1B_H),$$
$$\alpha_3 = \sin\psi, \quad \beta_3 = -\cos\psi$$
$$W_4 = 2\Im\{B_{Y'}(\omega = 2\omega_{sp})\}/(G_1B_H),$$
$$\alpha_4 = -\cos\psi, \quad \beta_4 = -\sin\psi.$$

The above set of equations can be solved by performing a multivariate least squares inversion. We once again use the iterative procedure outlined above to further improve the parameter estimates.

Finally, the fifth group of equations comprises (16b) and (16c). In solving this set of equations, one must remember that φ_3 appears only in combination with $\Delta\theta_3$ as $\cos\varphi_3\Delta\theta_3$ and $\sin\varphi_3\Delta\theta_3$. These quantities are small and can be solved for iteratively as above. Then, $\Delta\theta_3$ and φ_3 are calculated from $\cos\varphi_3\Delta\theta_3$ and $\sin\varphi_3\Delta\theta_3$. Thus, equations (16b) and (16c) are collected into

$$P_{j=1,2} = \cos\varphi_3\Delta\theta_3\gamma_j + \sin\varphi_3\Delta\theta_3\delta_j \tag{21}$$

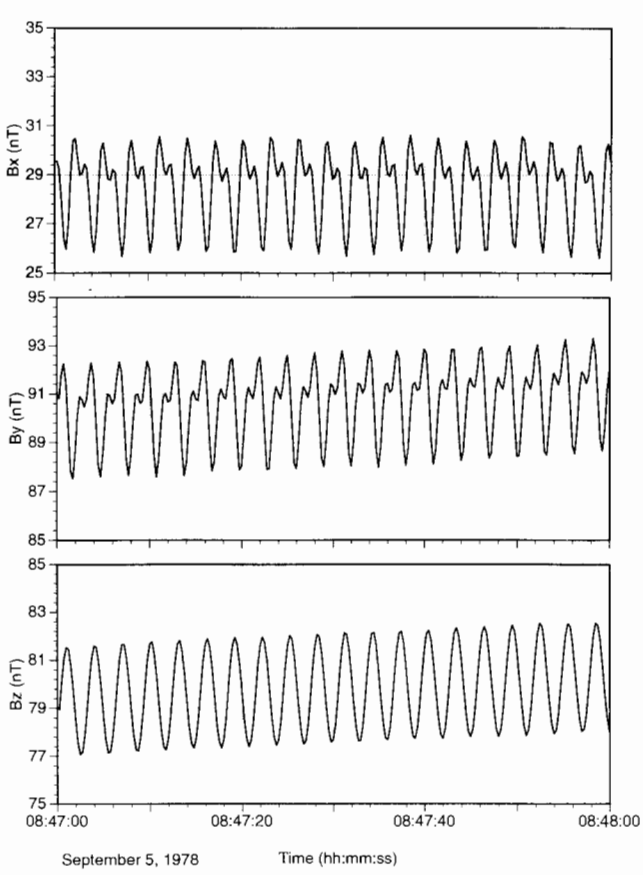

Fig. 1. A segment of the despun uncalibrated magnetic data collected by the ISEE-2 spacecraft in the inner magnetosphere.

where

$$P_1 = \Re\{B_{Z'}(\omega = \omega_{sp})\}/(G_3B_H),$$
$$\gamma_1 = \cos\psi, \ \delta_1 = \sin\psi$$
$$P_2 = \Im\{B_{Z'}(\omega = \omega_{sp})\}/(G_3B_H),$$
$$\gamma_2 = -\sin\psi, \ \delta_2 = \cos\psi. \tag{22}$$

Equation (21) can be solved in the same way as (20).

V. A TEST OF THE TECHNIQUE

We have successfully applied the technique on magnetometer data obtained from the ISEE 1 and 2 and the Galileo spacecraft. The technique has proven to be extremely robust because the coherent nature of the first and second spin harmonics allows us to distinguish them easily from the mainly low-coherence background produced by geophysical signals. In this section, we present results

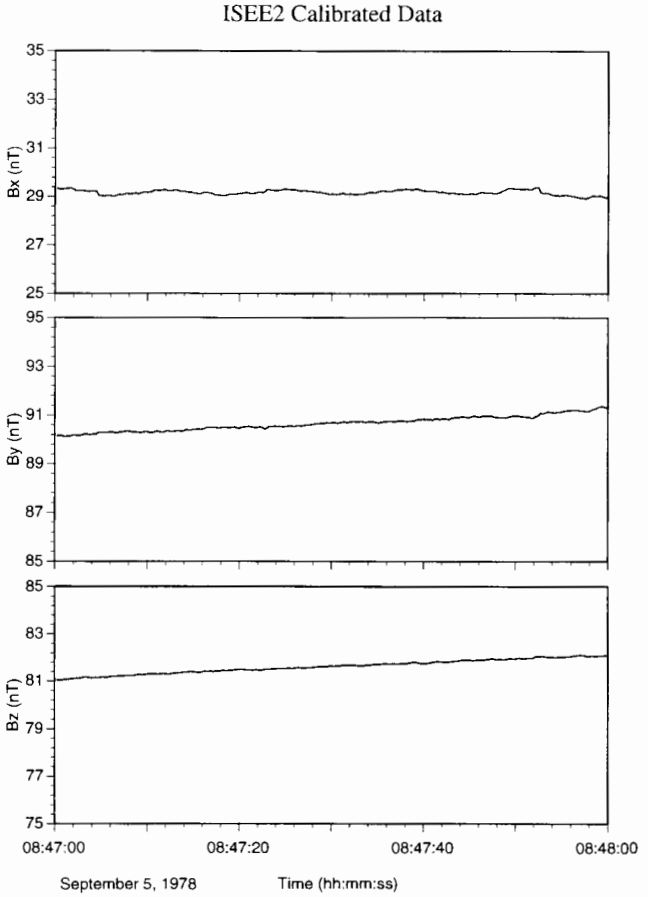

Fig. 2. The same segment of data after calibration. Notice that the spin harmonics in all three of the components have been reduced to the background level of the noise.

from a calibration performed on an ISEE 2 data set from September 5, 1978. The data were obtained from an inbound pass when the spacecraft was in the inner magnetosphere and measured a large range of magnetic field values. We used fourteen datasets, each approximately of three minutes duration. We used the discrete Fourier transform (DFT) technique to calculate the Fourier transform because, unlike the FFT, it allows us to perform the integration over an integral number of spin cycles so that the estimates of the real and imaginary parts of the spin harmonics can be obtained very accurately. The calibration required less than a minute of CPU time on a Sun SparcStation 20. The calibration parameters obtained from the calibration are listed in Table II. In order to show how well the technique removes the first and second harmonic signals from the despun data, we show a segment of the despun uncalibrated data in Fig. 1 and the same segment after calibration in Fig. 2. The calibrated data do not contain any enhanced power at spin harmonics. The dynamic spectra of the three components obtained from the uncalibrated despun data clearly show large first and second harmonics in the spin plane components and a large first harmonic in the spin axis component (Fig. 3). The values of the spin harmonics in the dynamic spectra of the calibrated despun data are near the background levels (Fig. 4).

VI. Discussion

Our experience with the above technique has shown that, under ideal conditions, the elevation and mutual angles can be calculated with a precision of better than 0.01 degree. The two spin plane offsets can be obtained with a precision of better than 0.05 nT, and the mutual gain mismatch between sensors 1 and 2 can be obtained with an accuracy of better than 0.1%. Even under adverse conditions, the angles can be calculated with a precision of better than 0.1 degree routinely. The main prerequisites for obtaining a good calibration are: 1) among them, the data segments should cover a large range of magnetic field values (equations (14)–(16) show that the amplitudes of the three components of the magnetic field modulate the amplitudes of the spin harmonics); 2) the background noise in the data sets should be small so that the spin harmonics can be distinguished from the background easily; and 3) the calibration parameters being calculated should have remained constant during the time when the calibration data were collected. All three conditions are easily met by the data collected by fluxgate mangetometers in the Earth's magnetosphere.

References

[1] M. W. Dunlop, "Review of the Cluster orbit and separation strategy: Consequences for measurements," in *Proc. Int. Workshop Space Plasma Phys. Investigat. Cluster Regatta*, Graz, Austria, ESA SP-306, 1990.

[2] M. W. Dunlop, A. Balogh, D. J. Southwood, R. C. Elphic, K.-H. Glassmeier, and F. M. Neubauer, "Configurational sensitivity of multipoint magnetic field measurements," in *Proc. Int. Workshop Space Plasma Phys. Investigat. Cluster Regatta*, Graz, Austria, ESA SP-306, 1990.

[3] K. K. Khurana, E. L. Kepko, M. G. Kivelson, and R. C. Elphic, "Accurate calculation of magnetic field gradients from four point vector measurements—Part II: Use of natural constraints on vector data obtained from four spinning spacecraft," to be published.

[4] W. M. Farrell, R. F. Thompson, R. P. Lepping, and J. B. Byrnes, "A method of calibrating magnetometers on a spinning spacecraft," *IEEE Trans. Magn.*, vol. 31, p. 966, 1995.

Emil (Larry) Kepko received the B.S. degree in astrophysics from the University of California, Los Angeles in 1993. He is currently a second year graduate student in the Department of Earth and Space Sciences at UCLA.

His current research interests include FTE's and the structure of the Earth's magnetopause. This is his first published paper.

Krishan K. Khurana received the B.S. degree from Delhi University, India, the M.S. degree from Osmania University, India and the Ph.D. degree from Durham University, U.K.

Since 1985, he has been working as a space scientist at the Institute of Geophysics and Planetary Physics at University of California, Los Angeles. He is currently investigating the structure of the planetary bow shocks, the plasma convection in the Earth's magnetosphere, flux rope type structures encountered in space plasmas and the magnetic field of Jupiter. He has been involved with the analysis of spacecraft data from Voyager, ISEE and Galileo spacecraft.

Margaret Kivelson received the Ph.D. degree from Harvard University in 1957.

She is Professor of Space Physics, Department of Earth and Space Sciences and Institute of Geophysics and Planetary Physics, UCLA, and is

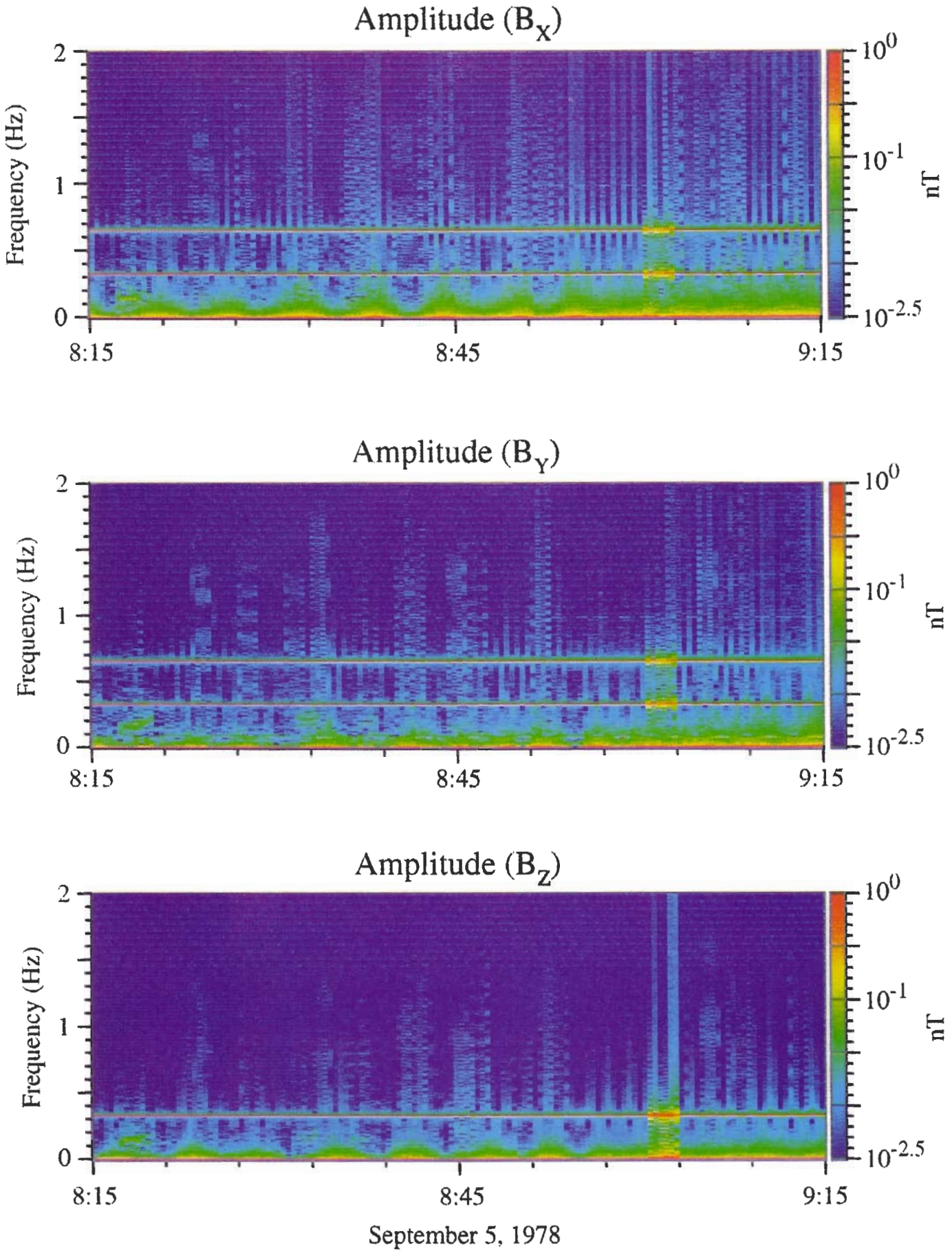

Fig. 3. The dynamic spectra of the uncalibrated data shows the presence of large signals at the first and second spin harmonics in the spin plane components (B_X and B_Y) and the first harmonic in the spin axis component (B_Z).

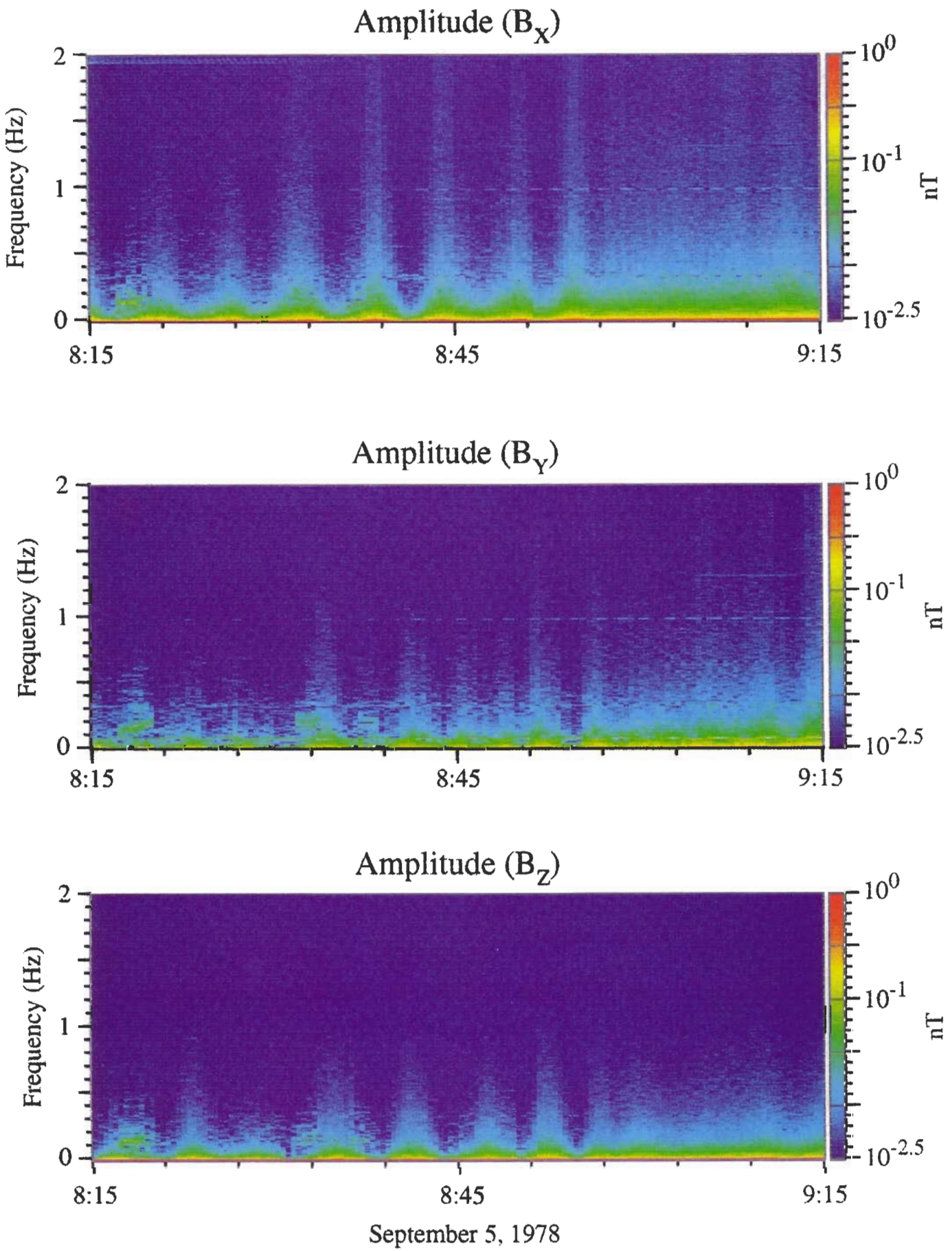

Fig. 4. The dynamic spectra of the calibrated data.

the Principal Investigator on the Magnetometer Investigation for the Galileo Mission. Her research consists of both theoretical and empirical investigations. Specific topics include the large-scale dynamics and electric fields of the magnetospheres of Earth and Jupiter, interactions of flowing plasmas with satellites of outer planetary magnetosphere, the formation of shocks in differing plasma conditions, and the role of the interchange instability in rotating plasmas.

Dr. Kivelson is a Fellow of the American Association for the Advancement of Science (1988), and the American Geophysical Union (1992). Her honors and awards include: the Muses Woman of the Year award of the California Museum of Science, Industry (1979); the Radcliffe Graduate Society Medal (1983); and the Harvard University 350th Anniversary Alumni Medal (1986).

R. C. Elphic received the Ph.D. degree in Geophysics and Space Physics from the University of California, Los Angeles in 1982.

He is presently a staff member in the Space and Atmospheric Sciences group at Los Alamos National Laboratory, and where he is involved in the design and development of spaceflight instrumentation for future NASA and DOE missions.

Dr. Elphic is a past collaborator on the ISEE, Pioneer Venus Orbiter, and AMPTE missions, and is a co-investigator on the Cluster magnetometer team. He has authored or co-authored 116 papers in journals and books.

C. T. Russell received the B.Sc. degree in physics from the University of Toronto in 1964 and the Ph.D. in space physics from UCLA in 1968. In 1969 he joined the research staff of the UCLA Institute of Geophysics and Planetary Physics.

In 1982 he joined the faculties of both the Institute of Geophysics and the Department of Earth and Space Sciences.

Dr. Russell is a Fellow of the American Geophysical Union and the American Association for the Advancement of Science. He is an Associate of the Royal Astronomical Society. He is a member of the American Astronomical Society. His instruments have been selected for flight on ISEE-1 and -2, and Pioneer Venus and the ISTP/Polar mission. He has served as a co-investigator on the magnetic fields investigations on the Apollo 15 and 16 subsatellites, Galileo, VEGA, Phobos, Mars 96 and Cassini missions and he is an interdisciplinary scientist on the Galileo mission. He has been an editor of EOS, the weekly newspaper of the AGU, has served as editor of 14 different books and is presently an editor of Planetary and Space Science and on the editorial board of Space Science Reviews. He is the author of over 725 articles in journals and books on various aspects of space physics.